




Article

Auroselenide, AuSe, a new mineral from Maletoyvayam deposit, Kamchatka peninsula, Russia

Nadezhda Tolstykh¹, Anatoly Kasatkin^{2*} , Fabrizio Nestola³, Anna Vymazalová⁴, Atali Agakhanov², Galina Palyanova¹ and Vladimir Korolyuk¹

¹Sobolev Institute of Geology and Mineralogy, SB RAS, prosp. Akademika Koptyuga 3, 630090 Novosibirsk, Russia; ²Fersman Mineralogical Museum of the Russian Academy of Sciences, Leninsky Prospekt 18-2, 119071 Moscow, Russia; ³Dipartimento di Geoscienze, Università di Padova, Via Gradenigo 6, I-35131, Padova, Italy; and ⁴Czech Geological Survey, Geologická 6, 152 00 Prague 5, Czech Republic

Abstract

Auroselenide, ideally AuSe, is a new mineral from the Gaching ore occurrence of the Maletoyvayam deposit, Kamchatka peninsula, Russia. It occurs as anhedral grains up to 0.05 × 0.02 mm and as intergrowths up to 0.06 mm with maletoyvayamite–tolstykhite-series minerals, enclosed in native gold. Other associated minerals include pyrite, calaverite, fischerite, gachingite, tetrahedrite-group minerals [stibiogoldfieldite, its As-analogue, tennantite-(Cu) and tetrahedrite-(Zn)], tripuhyite, minerals of the famatinite–luzonite and selenium–tellurium series, paraganajuatite, petrovskaita, součekite and tiemannite. Auroselenide is bluish-grey, opaque with metallic lustre and grey streak. It is brittle and has an uneven fracture. $D_{\text{calc}} = 9.750 \text{ g/cm}^3$. In reflected light, auroselenide is grey with a bluish shade. Bireflectance is very weak. No pleochroism and internal reflections are observed. In crossed polars, it is strongly anisotropic with bluish to brownish rotation tints. The reflectance values for wavelengths recommended by the Commission on Ore Mineralogy of the International Mineralogical Association are ($R_{\text{min}}/R_{\text{max}}$, %): 28.4/31.5 (470 nm), 30.2/33.3 (546 nm), 31.9/34.9 (589 nm) and 34.3/37.3 (650 nm). The principal bands in the Raman spectrum of auroselenide are at 93, 171, 200, 210 and 325 cm^{-1} . The empirical formula calculated on the basis of 2 atoms per formula unit is $(\text{Au}_{0.98}\text{Ag}_{0.01})_{\Sigma 0.99}(\text{Se}_{0.79}\text{S}_{0.17}\text{Te}_{0.05})_{\Sigma 1.01}$. Auroselenide is monoclinic, space group $C2/m$, $a = 8.319(1)$, $b = 3.616(1)$, $c = 6.276(2)$ Å, $\beta = 104.54(2)^\circ$, $V = 182.74(5)$ Å³ and $Z = 4$. The strongest lines of the powder X-ray diffraction pattern [d , Å (I , %) (hkl)] are: 4.015 (54) (200); 3.033 (25) ($\bar{1}11$, 002); 2.780 (100) ($\bar{2}02$, 111); 2.172 (20) ($\bar{3}11$, 310); and 1.811 (25) ($\bar{1}13$). Auroselenide is the natural analogue of synthetic β -AuSe. The structural identity between them is confirmed by powder X-ray diffraction and Raman spectroscopy. The mineral is named according to its composition, as a combination of the main elements Au (*aurum*) and Se (*selenium*).

Keywords: auroselenide, new mineral, Raman spectroscopy, chemical composition, powder X-ray diffraction, synthetic β -AuSe, Maletoyvayam deposit, Kamchatka peninsula

(Received 21 October 2022; accepted 5 December 2022; Accepted Manuscript published online: 19 December 2022; Associate Editor: František Laufek)

Introduction

This article continues a series of papers describing new mineral species of the Au–Te–Se–S system discovered at the Gaching ore occurrence of the Maletoyvayam deposit, Kamchatka peninsula, the Far East of the Russian Federation (60°19′51.87″N, 164°46′25.65″E). Three new minerals were reported previously: maletoyvayamite, $\text{Au}_3\text{Se}_4\text{Te}_6$ (Tolstykh *et al.*, 2020), gachingite, $\text{Au}(\text{Te}_{1-x}\text{Se}_x)$, $0.2 \approx x \leq 0.5$ (Tolstykh *et al.*, 2022a) and tolstykhite $\text{Au}_3\text{S}_4\text{Te}_6$ (Kasatkin *et al.*, 2023). Auroselenide (pronounced a:u-ro-se-le-naid; Cyrillic – ауроселенид) described below is, thus, the fourth mineral discovered at the deposit.

Two synthetic polymorphs of gold selenide (α -AuSe and β -AuSe) have been known for a long time and are well studied

in solid-state chemistry and experimental mineralogy (Cranton and Heyding, 1968; Rabenau *et al.*, 1971; Cretier and Wieggers, 1973; Rabenau and Schulz, 1976; Ettema *et al.*, 1994; Lee and Jung, 1999; Wagner *et al.*, 2010; Feng and Taskinen, 2014; Palyanova *et al.*, 2016a, 2016b, 2019, 2020, 2022; Machogo *et al.*, 2019 etc.). However, natural AuSe has now been found in the Maletoyvayam deposit and, as shown below, it corresponds to the β -AuSe polymorph. It was first reported by Tolstykh *et al.* (2018) as an unnamed phase.

Auroselenide is named according to its composition, as a combination of the main elements Au (*aurum*) and Se (*selenium*). The new mineral, its name and symbol (Ause) have been approved by the Commission on New Minerals, Nomenclature and Classification of the International Mineralogical Association (IMA2022-052; Tolstykh *et al.*, 2022b). The holotype specimen is deposited in the collections of the Sobolev Institute of Geology and Mineralogy SB RAS, Central Siberian Geological Museum, Novosibirsk, Russian Federation, catalogue number IV-6/1.

*Author for correspondence: Anatoly Kasatkin, Email: anatoly.kasatkin@gmail.com

Cite this article: Tolstykh N., Kasatkin A., Nestola F., Vymazalová A., Agakhanov A., Palyanova G. and Korolyuk V. (2023) Auroselenide, AuSe, a new mineral from Maletoyvayam deposit, Kamchatka peninsula, Russia. *Mineralogical Magazine* 87, 284–291. <https://doi.org/10.1180/mgm.2022.137>

Table 1. Chemical composition of rare ore minerals identified in the association with auroselenide (our data).

	Clv ¹	Fam ¹	Fis	Gac	Luz ¹	Mty	Pgi ¹	Pvk ¹	Sče ¹	Tls	Tetrahedrite-group minerals			
											Sbgf	Asgf	Tnt-Cu	Ttr-Zn
wt. %														
Fe	–	–	–	–	–	–	–	–	–	–	0.80	0.99	0.35	1.22
Cu	–	44.15	–	–	47.02	–	–	–	11.98	–	43.38	44.84	46.74	39.20
Zn	–	–	–	–	–	–	–	–	–	–	–	0.11	–	5.39
Ag	–	–	47.67	–	–	–	–	32.06	–	–	–	–	–	1.61
Au	42.10	–	27.90	65.73	–	37.55	–	56.80	–	39.57	–	–	–	–
Pb	–	–	–	–	–	–	–	–	39.28	–	–	–	–	–
As	–	5.16	–	–	16.09	–	–	–	–	–	4.48	6.45	13.66	2.40
Sb	–	20.61	–	–	4.48	–	–	–	22.41	–	10.53	6.53	5.11	23.70
Te	57.33	–	2.94	22.22	–	48.12	2.54	–	–	49.71	11.14	12.95	3.65	1.81
Bi	–	–	–	–	–	–	63.77	–	–	–	–	–	0.90	–
S	–	28.72	–	–	31.41	3.43	–	9.49	11.85	6.65	21.18	23.53	25.20	24.81
Se	–	1.70	21.35	12.21	–	11.76	33.75	1.26	14.22	4.50	7.75	3.01	4.13	–
Total	99.43	100.34	99.86	100.16	99.00	100.86	100.06	99.61	99.74	100.43	99.26	99.37	99.74	100.14
Atoms per formula unit														
Based on:	3	8	6	2	8	13	5	3	6	13	As + Sb + Te + Bi = 4			
Fe	–	–	–	–	–	–	–	–	–	–	0.25	0.29	0.10	0.36
Cu	–	3.00	–	–	3.00	–	–	–	1.02	–	11.70	11.71	11.44	10.23
Zn	–	–	–	–	–	–	–	–	–	–	–	0.03	–	1.37
Ag	–	–	3.02	–	–	–	–	0.99	–	–	–	0.15	–	0.25
Au	0.97	–	0.97	1.01	–	3.01	–	0.96	–	3.05	–	–	–	–
Pb	–	–	–	–	–	–	–	–	1.02	–	–	–	–	–
As	–	0.30	–	–	0.87	–	–	–	–	–	1.02	1.43	2.84	0.53
Sb	–	0.73	–	–	0.15	–	–	–	0.99	–	1.48	0.89	0.65	3.23
Te	2.03	–	0.16	0.53	–	5.95	0.13	–	–	5.92	1.50	1.68	0.44	0.24
Bi	–	–	–	–	–	–	2.03	–	–	–	–	–	–	0.07
S	–	3.87	–	–	3.98	1.69	–	0.99	1.99	3.15	11.32	12.18	12.22	12.84
Se	–	0.09	1.85	0.47	–	2.35	2.84	0.05	0.97	0.87	1.68	0.63	0.81	–

Key: Asgf – As-analogue of stibio-goldfieldite; Clv – calaverite; Fam – famatinite; Fis – fischesserite; Gac – gachingite; Luz – luzonite; Mty – maletoyvayamite; Pgi – paraganajuaitite; Pvk – petrovskaitite; Sbgf – stibio-goldfieldite; Sče – součekite; Tls – tolstykhite; Tmn – tiemannite; Tnt-Cu – tennantite-(Cu); Ttr-Zn – tetrahedrite-(Zn). Mineral symbols are in accordance with Warr (2021).

– = below detection limits.

¹The identification of these minerals is confirmed by XRD data: Clv – monoclinic, $a = 8.744(1)$, $b = 4.4252(8)$, $c = 10.138(4)$ Å, $\beta = 125.56(2)^\circ$ and $V = 319.1(1)$ Å³ (calculated from PXRD data); Fam-Luz – tetragonal, $a = 5.2888(5)$, $c = 10.658(1)$ Å and $V = 298.13(6)$ Å³ (calculated from PXRD data); Pgi – trigonal, $a = 4.119(2)$, $c = 28.55(2)$ Å and $V = 419.4(4)$ Å³ (calculated from PXRD data); Pvk – monoclinic, $a = 4.9487(4)$, $b = 6.623(1)$, $c = 7.2515(7)$ Å, $\beta = 95.068(9)^\circ$ and $V = 236.74(4)$ Å³ (calculated from PXRD data); Sče – orthorhombic, $a = 8.15(4)$, $b = 8.50(7)$, $c = 8.08(3)$ Å and $V = 560(6)$ Å³ (single-crystal XRD data)

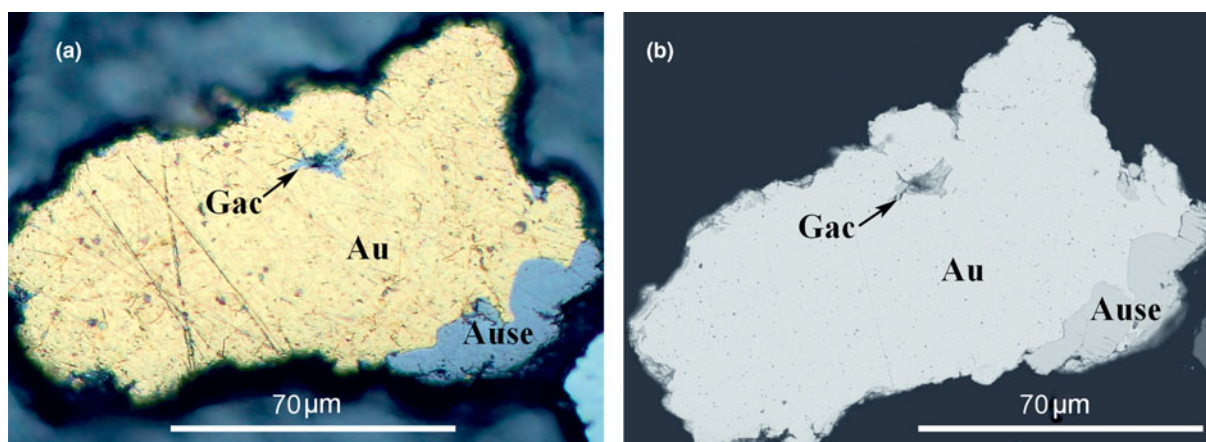


Fig. 1. Anhedronal grain (holotype, catalogue number IV-6/1) of auroselenide (Ause) in native gold (Au) with a small inclusion of gachingite (Gac): (a) photomicrograph in reflected light; and (b) back-scattered electron (BSE) image. This auroselenide grain is the largest found and was used to collect the Raman spectrum, reflectance dataset, chemical and XRD data.

Occurrence and mineral association

The Maletoyvayam deposit is located in the southwestern part of the Koryak Highland in the Far East of the Russian Federation. It belongs to the high-sulfidation type of epithermal deposits and is

confined to the Eocene–Oligocene Central Kamchatka volcanic belt ~1800 km long (Okrugin, 2003; Okrugin *et al.*, 2014; Tsukanov, 2015; Tolstykh *et al.*, 2018). Gaching, where all the new gold chalcogenides have been discovered, is one of the four ore occurrences comprising the Maletoyvayam deposit. A detailed

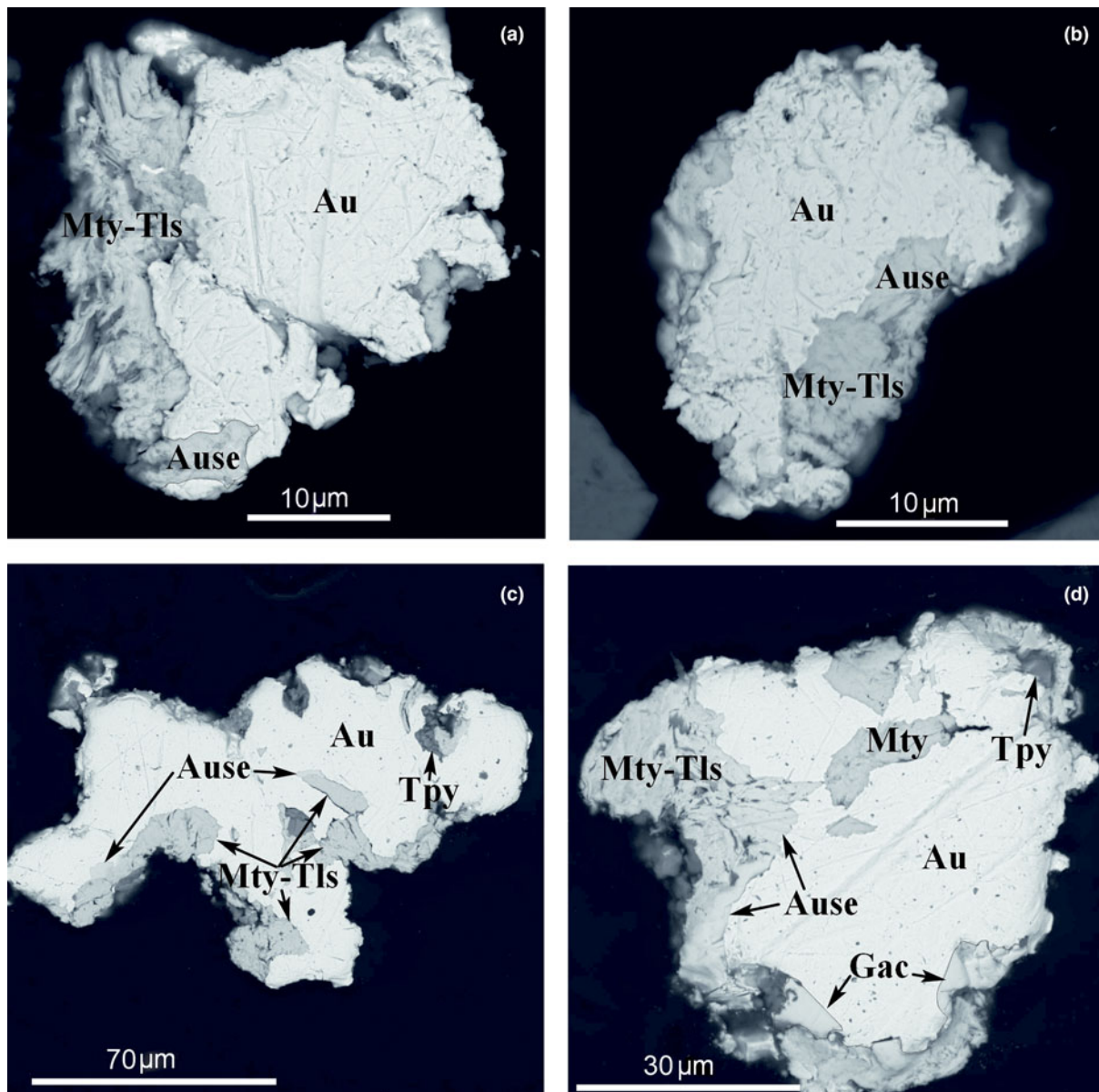


Fig. 2. Intergrowths of aurosenide (Ause) with minerals of maletoyvayamite (Mty) – tolstykhite (Tls) series, gachingite (Gac) and tripuhyite (Tpy) in native gold (Au). Polished section. Back-scattered electron images.

geological description of the Maletoyvayam deposit and Gaching ore occurrence can be found elsewhere (Kalinin *et al.*, 2012; Shapovalova *et al.*, 2019; Sidorov *et al.*, 2020; Tolstykh *et al.*, 2018, 2019, 2020, 2022a, 2022c; Kasatkin *et al.*, 2023).

The Maletoyvayam deposit is composed of andesites, tuffs and tuffaceous sandstones. The main gangue minerals are quartz, alunite and kaolinite. The primary ore minerals include pyrite and native gold. Apart from these species, aurosenide is associated with minerals of the maletoyvayamite–tolstykhite series, acanthite, anglesite, baryte, calaverite, tetrahedrite-group minerals of different compositions [stibio-goldfieldite, As-analogue of stibio-goldfieldite, tennantite-(Cu), tetrahedrite-(Zn)], tripuhyite, famatinite-luzonite-series minerals, fischerite, gachingite, paraganajuatite, petrovskite, selenium-tellurium-series minerals, součekite, tiemannite and several unnamed Ag–Au–Se and Au–Sb–Fe–O compounds. The chemical data and selected unit

cell parameters of some of the rare ore minerals identified within this study in association with aurosenide are given in Table 1.

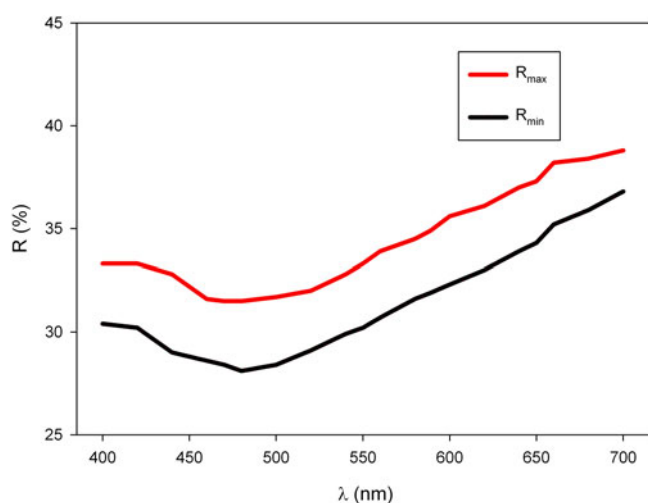
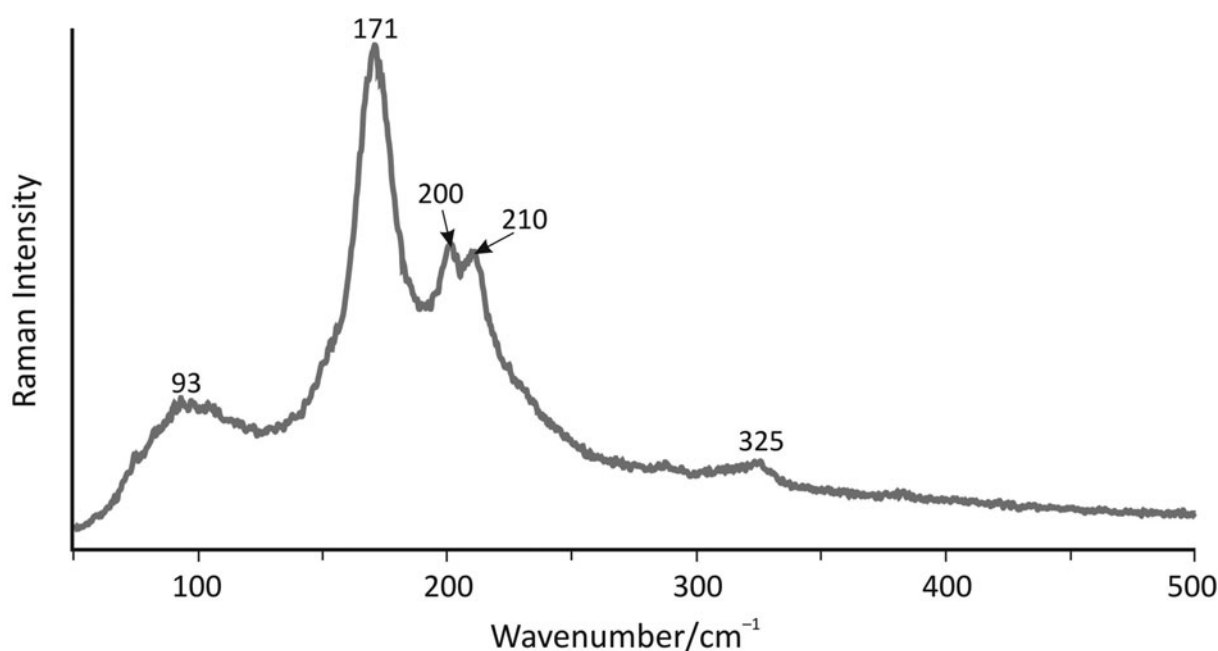
General appearance and physical properties

Aurosenide was found in polished sections containing a heavy-mineral concentrate from the Gaching occurrence prepared following the procedure described by Tolstykh *et al.* (2022a). The new mineral occurs as anhedral and drop-like grains up to 0.05×0.02 mm enclosed in native gold (Fig. 1). Some grains of aurosenide form complex intergrowths up to 0.06 mm with minerals of maletoyvayamite–tolstykhite solid-solution series, gachingite, famatinite, tripuhyite and native gold (Fig. 2).

Aurosenide is bluish-grey, opaque, with metallic lustre and a grey streak. Its tenacity is brittle and its fracture is uneven. No cleavage and parting are observed. The density calculated using

Table 2. Reflectance data (R , %) of auroselenide. The values required by the Commission on Ore Mineralogy are given in bold.

R_{\min}	R_{\max}	λ (nm)	R_{\min}	R_{\max}	λ (nm)
30.4	33.3	400	30.7	33.9	560
30.2	33.3	420	31.6	34.5	580
29.0	32.8	440	31.9	34.9	589
28.6	31.6	460	32.3	35.6	600
28.4	31.5	470	33.0	36.1	620
28.1	31.5	480	33.9	37.0	640
28.4	31.7	500	34.3	37.3	650
29.1	32.0	520	35.2	38.2	660
29.9	32.8	540	35.9	38.4	680
30.2	33.3	546	36.8	38.8	700

**Fig. 3.** Reflectance curves for auroselenide.**Fig. 4.** Raman spectrum of auroselenide.

the empirical formula and unit-cell volume obtained from powder X-ray diffraction (PXRD) data is 9.750 g/cm^3 .

In reflected light, auroselenide is grey with a bluish shade (Fig. 1a). Its bireflectance is very weak. No pleochroism and internal reflections are observed. In crossed polars, it is strongly anisotropic with bluish to brownish rotation tints. The reflectance values were measured in the air relative to a WTiC standard using a Microspectrophotometer UMSP 50 (Opton-Zeiss, Germany). Data are given in Table 2 and plotted in Fig. 3.

Raman spectroscopy

The Raman spectrum of auroselenide was collected at room temperature using Ramanor U-1000 spectrometer equipped with a Horiba DU420E – OE 323 “JobinYvon” detector, a MillenniaPro Spectra – Physics laser and an Olympus BX41 microscope. The nominal laser excitation wavelength was 532 nm. The data were collected using LabSpec software in the range of $50\text{--}1000 \text{ cm}^{-1}$. The experimental parameters were $100\times$ objective, 10 s exposure time, accumulation of 100 exposures and 1.5 mW laser power level. The spectral gap was $200 \mu\text{m}$ and, respectively, the spectral resolution was 2.09 cm^{-1} . The spectra were calibrated against the emission lines of a standard neon lamp; the peak position accuracy was up to $\pm 0.2 \text{ cm}^{-1}$.

The Raman spectrum of auroselenide is given in Fig. 4; the main bands observed are (in wavenumbers): 93, 171, 200, 210 and 325 cm^{-1} that are similar to the experimental and theoretical Raman spectra of synthetic AuSe provided by Machogo *et al.* (2019). The bands at 200 and 210 cm^{-1} could be assigned to A_{1g} symmetric stretching of the Au–Se bond and the one at 325 cm^{-1} to the B_{2g} antisymmetric stretching mode. The above bands correspond to the bands of 201 and 306 cm^{-1} , respectively, in the theoretical Raman spectrum of β -AuSe (Machogo *et al.*, 2019). The fact that observed bands in auroselenide are shifted to higher wavenumbers is probably due to the admixture of some S substituting Se in the composition of auroselenide (see

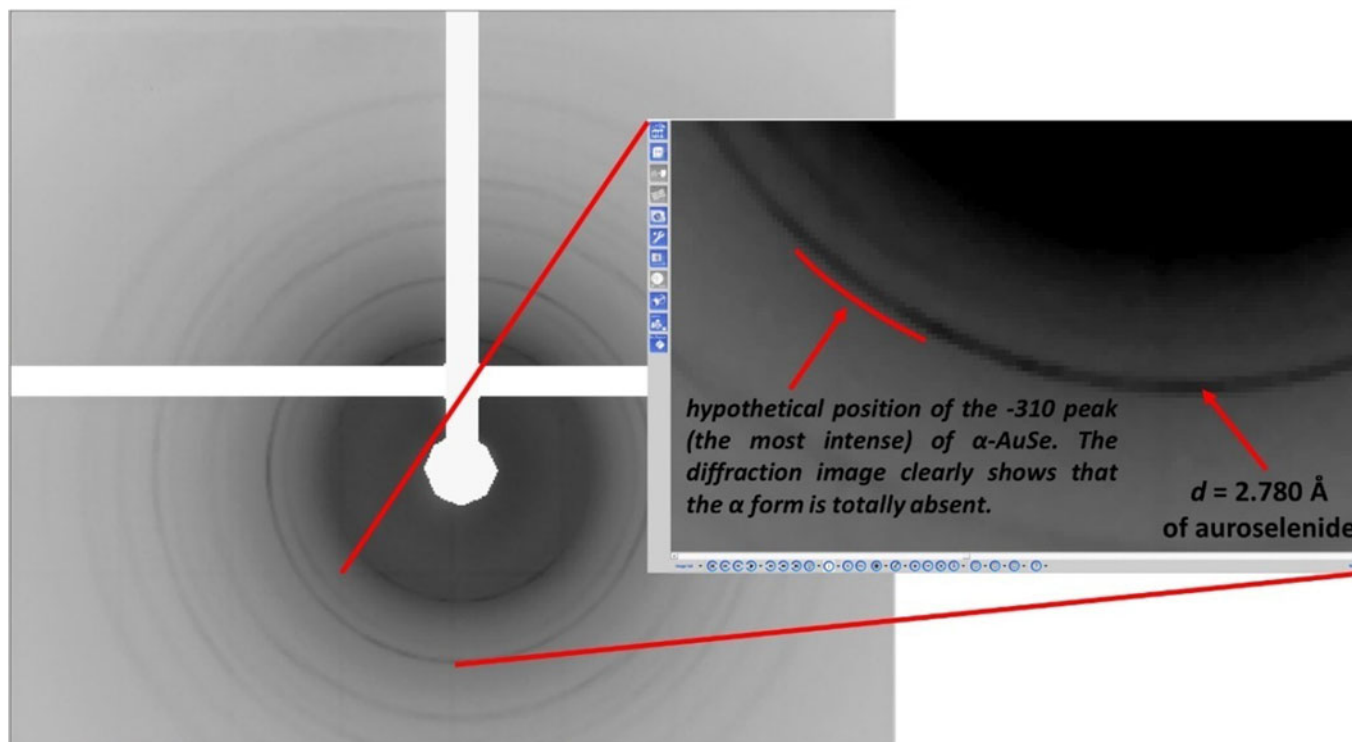


Fig. 5. Diffraction image of auroselenide.

below), as Hooke's Law predicts (Nakamoto, 1986). Analogous shifts have been reported as a consequence of S–Se substitution in permingeatite–famatinitite–luzonite (Škácha *et al.*, 2014), tetrahedrite–hakite (Škácha *et al.*, 2017), chalcostibite–příbramite (Sejkora *et al.*, 2018) and in tolstykhite–maletoyvayamite (Kasatkin *et al.*, 2023; Tolstykh *et al.*, 2020). The strong band at 171 cm^{-1} in auroselenide could be assigned to B_{1g} planar bending vibrations of the Au–Se bond. We must note, however, that Machogo *et al.* (2019) only attribute this band to the α -AuSe polymorph, whereas our PXRD data collected from the same grain used for Raman spectroscopic measurement definitively demonstrate the total absence of the α form (see Fig. 5). We were not able to assign the broad band at 93 cm^{-1} .

Chemical composition

Five quantitative chemical analyses were carried out with a JEOL JXA-8100 electron microprobe (wavelength dispersive spectroscopy mode with an accelerating voltage of 20 kV, a beam current

of 50 nA and a beam diameter of $1\text{ }\mu\text{m}$) at the Analytical Center for Multi-elemental and Isotope Research SB RAS (Sobolev Institute of Geology and Mineralogy SB RAS, Novosibirsk, Russia). Analytical lines were $K\alpha$ for S and $L\alpha$ for other elements. Peak counting times (CT) were 20 s for all elements; CT for each background was one-half of the peak time. Matrix correction by XPP software (Pouchou and Pichoir, 1985) was applied to the experimental data.

Analytical data and used standards are given in Table 3. Contents of other elements with atomic numbers higher than that of beryllium are below detection limits. The empirical formula based on 2 atoms per formula unit is $(\text{Au}_{0.98}\text{Ag}_{0.01})_{\Sigma 0.99}(\text{Se}_{0.79}\text{S}_{0.17}\text{Te}_{0.05})_{\Sigma 1.01}$. The ideal chemical formula is AuSe, which requires Au 71.40, Se 28.60, total 100 wt.%.

X-ray diffraction data

Single-crystal X-ray diffraction studies could not be carried out because of the absence of single crystals: grains of auroselenide are cryptocrystalline and inhomogeneous (see Fig. 5 showing typical diffraction rings of polycrystalline materials). Thus, the grain shown in Fig. 1, was extracted from the polished section and measured in powder diffraction mode using a Supernova single-crystal X-ray Rigaku-Oxford Diffraction diffractometer equipped with a Pilatus 200 K Dectris detector and a $\text{MoK}\alpha$ radiation X-ray micro-source (conditions: 50 kV, 0.12 mA and spot size of $\sim 0.12\text{ mm}$). The detector-to-sample distance was 68 mm. A standard phi scan mode as implemented in the Rigaku *CrysAlisPro* programme was used for the powder data collection. The data were collected over 360° around the phi axis with an exposure time of 140 s° . The observed d spacings (Table 4) showed a very good match with powder data reported in the ICDD Powder Diffraction File

Table 3. Chemical composition of auroselenide.

Constituent	Mean (wt.%)	Range	S.D. (σ)	Standard
Au	71.52	69.17–72.40	1.10	Au
Ag	0.46	0.14–0.92	0.28	Ag
Se	23.11	18.76–25.21	2.28	Bi_2Se_3
Te	2.29	1.04–3.87	1.03	AgTe_2
S	2.02	0.75–3.10	0.77	CuFeS_2
Total	99.40			

S.D. – standard deviation

Table 4. Powder X-ray data (d in Å, I in %) for auroselenide compared with that of the synthetic β -AuSe (ICSD #073669).

Auroselenide			Synthetic β -AuSe (ICSD #073669, PDF card #812227)				
d_{obs}	d_{calc}	I_{obs}	h	k	l	d_{calc}	I_{calc} (%)
4.015	4.026	54	2	0	0	4.0150	54
3.033	3.033	25	$\bar{1}$	1	1	3.0683	30
2.780	2.784	100	0	0	2	3.0092	13
2.172	2.174	20	$\bar{2}$	1	1	2.8088	48
			1	1	1	2.7834	100
			$\bar{3}$	1	1	2.1956	26
			3	1	0	2.1611	5
2.014	2.013	4	4	0	0	2.0075	5
1.911	1.914	16	$\bar{4}$	0	2	1.9347	11
			3	1	1	1.9035	18
1.811	1.811	25	$\bar{1}$	1	3	1.8130	24
1.653	1.651	13	$\bar{3}$	1	3	1.6673	12
			$\bar{2}$	2	1	1.6554	2
			1	1	3	1.6378	5
1.513	1.511	14	$\bar{5}$	1	1	1.5202	11
			0	0	4	1.5046	5
1.390	1.391	5	2	2	2	1.3917	5
			$\bar{3}$	1	4	1.3885	3

The strongest lines are in bold; ICSD – Inorganic Crystal Structure Database, <https://icsd.products.fiz-karlsruhe.de/>

database¹ (PDF) for synthetic β -AuSe (PDF cards #812227 and 200458). Unit cell parameters were calculated from the observed d spacings (using *UnitCell* by Holland and Redfern, 1997) and gave the following values: monoclinic, $C2/m$, $a = 8.319(1)$, $b = 3.616(1)$, $c = 6.276(2)$ Å, $\beta = 104.54(2)^\circ$, $V = 182.74(5)$ Å³ and $Z = 4$. These parameters are in a very good agreement with those of the synthetic phase β -AuSe (Rabenau and Schulz, 1976; ICSD² #073669, PDF card #812227, e.g. their data are: $a = 8.355(2)$, $b = 3.663(1)$, $c = 6.262(1)$ Å, $\beta = 106.03(2)^\circ$ and $V = 184.19$ Å³).

Crystal structure

As mentioned above, the AuSe crystalline compound exists in two different polymorphs, α -AuSe and β -AuSe (Rabenau and Schulz, 1976). Both are monoclinic with space group $C2/m$ but differ substantially in unit cell parameters. Those of α -AuSe are: $a = 12.202$, $b = 3.690$, $c = 8.433$ Å, $\beta = 103.15^\circ$ and $V = 369.74$ Å³ (Rabenau and Schulz, 1976). Table 4 and Fig. 5 clearly demonstrate that the identification of auroselenide as the natural analogue of β -AuSe is unambiguous due to the total absence of the strongest reflections of synthetic α -AuSe, such as 2.70, 2.74 and 8.21 Å (ICSD #073668, PDF card #812226). To date, the α -AuSe phase has not been found in nature yet.

Accordingly, the crystal structure of auroselenide corresponds to that of the synthetic β -AuSe phase (Rabenau and Schulz, 1976; Machogo *et al.*, 2019). Atomic coordinates and bond distances for β -AuSe are provided in Table 5.

The crystal structure of auroselenide shows two Au sites, Au1 with Au⁺ and Au2 with Au³⁺, and one Se site (Fig. 6). Au1 coordinates 2 Se whereas Au2 coordinates 4 Se. The bond distances are Au1–Se = 2.433 Å $\times 2$ and Au2–Se = 2.496 Å $\times 4$. As described by Rabenau and Schulz (1976) and Machogo *et al.* (2019), the crystal structures of both α - and β -AuSe consist of repeating units of a linearly bonded Au¹⁺ ion to two Se atoms and a Au³⁺ ion bonded

Table 5. Atomic coordinates and interatomic distances (d in Å) for synthetic β -AuSe (Rabenau and Schulz, 1976).

Atom	x	y	z	B_{iso}
Au1	0	0	0	2.1
Au2	0	$\frac{1}{2}$	$\frac{1}{2}$	1.3
Se	0.162(1)	0	0.732(1)	1.5
Interatomic distances				
Au1–Se	2.433(9) $\times 2$			
Au2–Se	2.496(9) $\times 4$			

to four Se atoms in a square planar geometry. Rabenau and Schulz (1976) describe the two structures in which essential Au–Se bonds form infinite rods parallel to the monoclinic b axis in α -AuSe and waved sheets parallel to (100) in auroselenide (β -AuSe). Rods and sheets are connected by weak Au–Au and Se–Se bonds in α -AuSe and by weak Au–Se bonds in auroselenide.

It is quite unusual that in all the synthesis runs, where α -AuSe and β -AuSe have been produced, these two polymorphs always coexist (see, e.g. Cranton and Heyding, 1968; Rabenau *et al.*, 1971; Machogo *et al.*, 2019; Palyanova *et al.*, 2022), whereas auroselenide does not show any trace of its α polymorph (see Fig. 5, Table 4) in natural conditions. This could be related to S and Te which substitute Se in not negligible amounts and probably stabilise the β polymorph.

Remarks on the origin

The formation of auroselenide implies special conditions: an abundant source of Au and Se deposited from acidic solutions in a highly oxidising environment (Tolstykh *et al.*, 2018, 2019; Shapovalova *et al.*, 2019). The detailed study of the composition of ore-forming fluid inclusions in quartz from Maletoyvayam deposit (Tolstykh *et al.*, 2022c) shows that they contain high concentrations (20 rel.%) of organic compounds (different hydrocarbons). The latter are able to accumulate and transport a significant amount of native elements, including Au and Se (Williams-Jones *et al.*, 2009; Migdisov *et al.*, 2017). The organic acids can also play an important role in the transport of gold. Au(I) forms strong complexes with cyanide (CN[−]) and thiocyanate (SCN[−]) ions – resulting from the decay of plants and algae and forming natural compounds such as Au(CN)^{2−} and Au(SCN)[−]. In acidic environments cyanide ions are oxidised to CO₂ and free nitrogen during the boiling of hydrothermal fluids (Karpov and Pavlov, 1976). This mechanism could be implemented at the Maletoyvayam deposit, as molecular nitrogen and CO₂ are found in fluid inclusions (Tolstykh *et al.*, 2022c).

The primary source of organic compounds and selenium could be bacteria and algae that were modified into organic matter of low maturity and then saturated the ore-forming fluids in Se and Au. The crystallisation of selenides is regulated by the H₂Se/H₂S ratio or at very high ratios of $f_{\text{Se}_2}/f_{\text{S}_2}$ in aqueous fluids (Hustor *et al.*, 1995; Yuningsih *et al.*, 2016; Tolstykh *et al.*, 2018). If this ratio is low, selenium enters sulfides as an isomorphic impurity replacing sulfur in minerals. Such a mechanism is observed at two other Kamchatka deposits, Baranyevskoe and Rodnikovoe, located to the south of Maletoyvayam and belonging to the same Central Kamchatka volcanogenic belt. However, much higher values of pH and f_{O_2} at Maletoyvayam leads to an increase in the above ratios and, consequently, to the formation of selenides (Simon *et al.*, 1997): the Au–S complexes are

¹International Centre for Diffraction Data, <https://www.icdd.com/pdfsearch/>

²Inorganic Crystal Structure Database, <https://icsd.products.fiz-karlsruhe.de/>

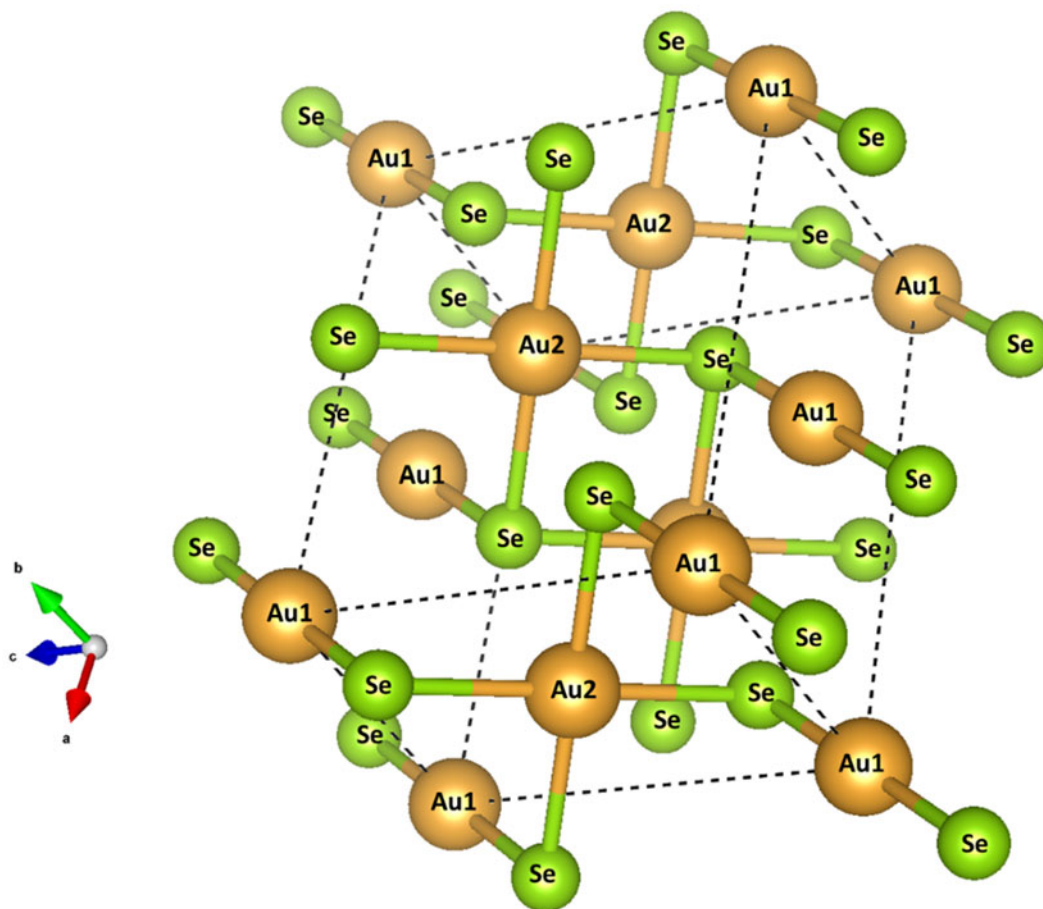


Fig. 6. The crystal structure of synthetic β -AuSe using Rabenau and Schulz (1976). The orientation is shown on the left side of the structure; the dashed lines represent the unit cell. Au1 is monovalent gold coordinating 2 Se, and Au2 is trivalent gold coordinating 4 Se. The ionic radii are not to scale. The structure was plotted using *Vesta 3* software (Momma and Izumi, 2011).

replaced successively by Au–S–Se (tolstykhite–maletoyvayamite-series minerals) and Au–Se (auroselenide).

Auroselenide does not form single grains in the host rock but always occurs in native gold, replacing it together with the minerals of maletoyvayamite–tolstykhite series, generally in the inner parts of the rims on gold grains (Fig. 2). Auroselenide belongs to a productive maletoyvayamite–quartz association and, as shown by studies of fluid inclusions in quartz (Sidorov *et al.*, 2020), forms in the temperature range of 245–225°C. At these temperatures $\log f_{\text{O}_2}$ is more than -27.3 and $\log f_{\text{Se}_2}$ ranges between -12.4 and -5.7 (Tolstykh *et al.*, 2018), typical for high-sulfidation type epithermal deposits (Hedenquist *et al.*, 2000; Hedenquist and Arribas, 2017) such as Maletoyvayam.

Acknowledgements. We thank Associate Editor František Laufek, Alexandre R. Cabral and an anonymous reviewer as well as the Principal Editor Stuart Mills for valuable comments. This research was carried out within the framework of the state assignment of the IGM SB RAS financed by the Ministry of Science and Higher Education of the Russian Federation and Grant Agency of the Czech Republic (project No. 22-26485S to A.V.). Part of the research related to the study of the conditions of auroselenide formation is performed with the financial support of the Russian Federation represented by the Ministry of Education and Science of Russia No. 13.1902.21.0018.

Competing interests. The authors declare none.

References

- Cranton G.E. and Heyding R.D. (1968) The gold/selenium system and some gold selenotellurides. *Canadian Journal of Chemistry*, **46**, 2637–2640.
- Cretier J.E. and Wieggers G.A. (1973) The crystal structure of the beta form of gold selenide, β -AuSe. *Materials Research Bulletin*, **8**, 1427–1430.
- Ettema A.R.H.F., Stegink T.A. and Haas, C. (1994) The valence of Au in AuTe₂ and AuSe studied by x-ray absorption spectroscopy. *Solid State Communications*, **90**, 211–213.
- Feng D. and Taskinen P. (2014) Thermodynamic stability of AuSe at temperature from (400 to 700) K by a solid state galvanic cell. *The Journal of Chemical Thermodynamics*, **71**, 98–102.
- Hedenquist J.W. and Arribas R.A. (2017) Epithermal ore deposits: first-order features relevant to exploration and assessment. *14th SGA Biennial Meeting, Quebec, Canada. Mineral Resources to Discover*, **1**, 47–50.
- Hedenquist J.W., Arribas A. and Gonzalez-Urien E. (2000) Exploration for epithermal gold deposits. *Reviews in Economic Geology*, **13**, 245–277.
- Holland T.J.B. and Redfern S.A.T. (1997) Unit cell refinement from powder diffraction data: the use of regression diagnostics. *Mineralogical Magazine*, **61**, 65–77.
- Hustor D.L., Sieb S.H. and Suterb G.F. (1995) Selenium theoretical and its importance to the study of ore genesis: the basis and its application to volcanic-hosted massive sulfide deposits using pixeprobe analysis. *Nuclear Instruments and Methods in Physics Research*, **104**, 476–480.
- Kalinin K.B., Andreeva E.D. and Yablokova D.A. (2012) Textures and structures of Jubilee ore occurrence (Maletoyvayam ore field). Pp. 39–48 in: *Materials XI Regional youth scientific conference "The Natural Environment of Kamchatka"*. Petropavlovsk-Kamchatsky, Russia [in Russian].

- Karpov G.A. and Pavlov A.L. (1976) *Uzon-Geyser Hydrothermal Small Ore-Forming System of Kamchatka*. Science (V.A. Kuznetsov, editor). Novosibirsk, Russia, 88 pp. [in Russian].
- Kasatkin A.V., Nestola F., Plášil J., Sejkora J., Vymazalová A. and Škoda R. (2023) Tolstykhite, $\text{Au}_3\text{S}_4\text{Te}_6$, a new mineral from Maletoyvayam deposit, Kamchatka peninsula, Russia. *Mineralogical Magazine*, **87**, 34–39, <https://doi.org/10.1180/mgm.2022.109>.
- Lee W. and Jung D. (1999) Electronic structure study of gold selenides. *Bulletin of the Korean Chemical Society*, **20**, 147–150.
- Machogo F.E.L., Mthimunya M., Sithole K.R.K., Tetyana P., Phao N., Ngubeni G.N., Mlambo M., Mduli P.S., Shumbula P.M. and Moloto N. (2019) Elucidating the structural properties of gold selenide nanostructures. *New Journal of Chemistry*, **43**, 5773.
- Migdisov A.A., Guo X., Xu H., Williams-Jones A.E., Sun C.J., Vasyukova O., Sugiyama I., Fuchs S., Pearce K. and Roback R. (2017) Hydrocarbons as ore fluids. *European Association of Geochemistry, Geochemical Perspectives. Letters*, **5**, 47–52.
- Momma K. and Izumi F. (2011) VESTA 3 for three-dimensional visualization of crystal, volumetric and morphology data. *Journal of Applied Crystallography*, **44**, 1272–1276.
- Nakamoto K. (1986) *Infrared and Raman Spectra of Inorganic and Coordination Compounds*. John Wiley and Sons, New York, USA.
- Okrugin V.M. (2003) New data on the age and genesis of epithermal deposits of transition zone continent-ocean (Pacific Northwest). Pp. 39–41 in: *Geodynamics, Magmatism and Metallogeny of Continental Margins of the North Pacific*. Materials of the XIIth Conference “Annual Meeting of the North-Eastern Branch of the WMO”. Magadan, Russia [in Russian].
- Okrugin V.M., Andreeva E.D., Etschmann B., Pring A., Li K., Zhao J., Griffins G., Lumpkin G.R., Triani G. and Brugger J. (2014) Microporous gold: Confirmation of Au-replacing textures from nature. *American Mineralogist*, **99**, 1171–1175.
- Palyanova G.A., Seryotkin Y.V., Bakakin V.V. and Kokh K.A. (2016a) Sulfur-selenium isomorphous substitution in the $\text{AgAu}(\text{S},\text{Se})$ series. *Journal of Alloys and Compounds*, **664**, 385–391.
- Palyanova G.A., Seryotkin Y.V., Kokh K.A. and Bakakin V.V. (2016b) Isomorphism and solid solutions among Ag- and Au-selenides. *Journal of Solid State Chemistry*, **241**, 157–163.
- Palyanova G.A., Tolstykh N.D., Zinina V.Yu., Kokh K.A., Seryotkin Yu.V. and Bortnikov N.S. (2019) Synthetic gold chalcogenides in the Au–Te–Se–S system and their natural analogs. *Doklady Earth Sciences*, **487**, 929–934 [in Russian].
- Palyanova G., Mikhlin Y., Zinina V., Kokh K., Seryotkin Y. and Zhuravkova T. (2020) New gold chalcogenides in the Au–Te–Se–S system. *Journal of Physics and Chemistry of Solids*, **138**, 109276.
- Palyanova G., Beliaeva T., Kokh K., Seryotkin Y., Moroz T. and Tolstykh N. (2022) Characterization of synthetic and natural gold chalcogenides by electron microprobe analysis, X-ray powder diffraction, and Raman spectroscopic methods. *Journal of Raman Spectroscopy*, **53**, 1012–1022.
- Pouchou J.L. and Pichoir F. (1985) “PAP” ($\varphi\rho Z$) procedure for improved quantitative microanalysis. Pp. 104–106 in: *Microbeam Analysis* (J.T. Armstrong, editor). San Francisco Press, San Francisco.
- Rabenau A. and Schulz, H. (1976) The crystal structures of α -AuSe and β -AuSe. *Journal of the Less-Common Metals*, **48**, 89–101.
- Rabenau A., Rau H. and Rosenstein, G. (1971) Phase relations in the gold-selenium system, *Journal of the Less-Common Metals*, **24**, 291–299.
- Sejkora J., Buixaderas E., Škácha P. and Plášil J. (2018) Micro-Raman spectroscopy of natural members along CuSbS_2 – CuSbSe_2 join. *Journal of Raman Spectroscopy*, **49**, 1364–1372.
- Shapovalova M., Tolstykh N. and Bobrova O. (2019) Chemical composition and varieties of sulfosalts from gold mineralization in the Gaching ore occurrence (Maletoyvayam ore field). *IOP Conf. Series: Earth and Environmental Science*, **319**, 012019.
- Sidorov E.G., Borovikov A.A., Tolstykh N.D., Bukhanova D.S., Palyanova G.A. and Chubarov V.M. (2020) Gold mineralization at the Maletoyvayam deposit (Koryak Highland, Russia) and physicochemical conditions of its formation. *Minerals*, **10**, 1093.
- Simon G., Kesler S.E. and Essene E.J. (1997) Phase relations among selenides, sulfides, tellurides, and oxides: II. Applications to selenide-bearing ore deposits. *Economic Geology*, **92**, 468–484.
- Škácha P., Buixaderas E., Plášil J., Sejkora J., Goliáš V. and Vlček V. (2014) Permingeaitite, Cu_3SbSe_4 , from Příbram (Czech Republic): Description and Raman spectroscopy investigations of the luzonite-subgroup of minerals. *The Canadian Mineralogist*, **52**, 501–511.
- Škácha P., Sejkora J. and Plášil J. (2017) Selenide mineralization in the Příbram uranium and base-metal district (Czech Republic). *Minerals*, **7**, 91.
- Tolstykh N., Vymazalová A., Tuhý M. and Shapovalova M. (2018) Conditions of Au–Se–Te mineralization in the Gaching ore occurrence (Maletoyvayam ore field), Kamchatka, Russia. *Mineralogical Magazine*, **82**, 649–674.
- Tolstykh N., Palyanova G., Bobrova O. and Sidorov E. (2019) Mustard gold of the Gaching ore deposit (Maletoyvayam ore Field, Kamchatka, Russia). *Minerals*, **9**, 489.
- Tolstykh N.D., Tuhý M., Vymazalová A., Plášil J., Laufek F., Kasatkin A.V., Nestola F. and Bobrova O.V. (2020) Maletoyvayamite, $\text{Au}_3\text{Se}_4\text{Te}_6$, a new mineral from Maletoyvayam deposit, Kamchatka peninsula, Russia. *Mineralogical Magazine*, **84**, 117–123.
- Tolstykh N.D., Tuhý M., Vymazalová A., Laufek F., Plášil J. and Košek F. (2022a) Gachingite, $\text{Au}(\text{Te}_{1-x}\text{Se}_x)$ $0.2 \approx x \leq 0.5$, a new mineral from Maletoyvayam deposit, Kamchatka peninsula, Russia. *Mineralogical Magazine*, **86**, 205–213.
- Tolstykh N., Kasatkin A., Nestola F., Vymazalová A., Agakhanov A., Palyanova G. and Korolyuk V. (2022b) Auroselelide, IMA 2022-052. CNMNC Newsletter 69. *Mineralogical Magazine*, **86**, <https://doi.org/10.1180/mgm.2022.115>.
- Tolstykh N.D., Bortnikov N.S., Shapovalova M.O. and Shaparenko E.O. (2022c) The role of organic compounds in the formation of epithermal gold-silver deposits of Kamchatka, Russia. *Doklady Earth Sciences*, **507**, 13–20 [in Russian].
- Tsukanov N.V. (2015) Tectonic-stratigraphic terranes, Kamchatka active margins: structure, composition and geodynamics. *Proceedings of the annual conference “Volcanism and related processes”*. Petropavlovsk-Kamchatsky: IVS FEB RAS, 97–103.
- Wagner F.E., Palade P., Friedl J., Filoti G. and Wang N. (2010) ^{197}Au Mössbauer study of gold selenide, AuSe. *Journal of Physics, Conference Series*, **217**, 012039.
- Warr L.N. (2021) IMA-CNMNC approved mineral symbols. *Mineralogical Magazine*, **85**, 291–320.
- Williams-Jones A., Bowell R. and Migdisov A. (2009) Gold in solution. *Elements*, **5**, 281–287.
- Yuningsih E.T., Matsueda H. and Rosana M.F. (2016) Diagnostic genesis features of Au-Ag selenide-telluride mineralization of Western Java Deposits. *Indonesian Journal of Geosciences*, **3**, 67–76.